ADVANCED CONCEPTS FOR SEEDED FELS

Eugenio Ferrari*, Enrico Allaria, Elettra - Sincrotrone Trieste SCpA, Trieste, Italy

Abstract

The experiments enabled by ultrashort XUV/X-rays FELs, e.g. coherent control of quantum phenomena, nonlinear optics, etc., require the knowledge, and possibly the control, of the spectro-temporal content of individual pulses. While spatial coherence is also a property of FELs based on SASE, the capability of generating temporally coherent pulses is a distinctive feature of seeded FELs. Indeed, this is a natural consequence of the principle on which a seeded FEL relies: before emitting radiation, electrons interact with a coherent source, the seed, and, under given conditions, the latter transmits its coherence properties to the FEL light. In the following, we demonstrate the use of interferometry in the frequency domain to investigate the properties of the seeded FEL pulses. Moreover, we provide the first direct evidence of the temporal coherence of a seeded FEL working in the extreme ultraviolet spectral range and show the way to control the light generation process to produce Fourier-limited pulses.

INTRODUCTION

Seeded FELs have the potential to produce spatially and temporally fully coherent pulses [1]. However, the ability to generate fully coherent pulses and shape their spectro-temporal content with high stability on a shot-to-shot basis is extremely challenging, due to the difficulties in precisely controlling the light generation process [2]. In addition to amplification, several factors contribute to the evolution of the electric field during the FEL process. A linear frequency chirp $d\omega/dt$ in the seed affects the emission process, causing a broadening of the spectral envelope [3]. Furthermore, before interacting with the seed, electrons are accelerated and can acquire a time-dependent energy profile. A curvature $d^2\gamma(t)/dt^2$ in the electron energy $\gamma(t)$ produces the same effect as a linear frequency chirp in the seed [4,5] and causes an additional linear frequency offset during amplification due to varying $d\gamma(t)/dt$ along the electron beam [6]. The interplay between these effects determines the FEL temporal phase, which has an impact on the spectral content of the radiated light [7].

PHASE-LOCKED FEL PULSES

In a coherent control experiment, light pulses are used to guide the real-time evolution of a quantum system. This requires the coherence and the control of the pulses' electric-field carrier waves. In the following we demonstrate the generation of two time-delayed phase-locked XUV pulses from a seeded FEL. The pulses are produced by two seed replicas locked in phase. The adopted approach also provides a method to investigate the longitudinal coherence of a seeded FEL.

* eugenio.ferrari@psi.ch

Experimental Setup

The experiment was performed on FEL-1 [8] and exploits the capability of the seed laser to trigger and drive the FEL process and generate coherent and controllable XUV pulses.

Figure 1 shows the experimental setup for the generation of two time-delayed phase-locked pulses implemented at FERMI. The twin seed pulses are produced from a single pulse of the third harmonic of a Ti:Sa laser and temporally split into two pulses after transmission through a birefringent plate. The thickness of the birefringent plate and the group velocity difference for the two plate's orthogonal axes, rotated at 45° with respect to the laser polarization, determine the time delay τ between the two seed pulses. The polarization of both pulses is then adjusted to be parallel to the modulator one using adequate optical components. This ensures optimum seed-electron coupling in the modulator.

The relative phase between the carrier waves of the twin seed pulses $\Delta\phi_{seed}$ is controlled by fine tuning the incidence angle on the plate using a motorized rotation stage with minimum phase step of about $\lambda_{seed}/30$. The two seeds interact with the relativistic electron beam inside the modulator and give rise to a periodic energy modulation at the seed wavelength, which is confined to the position of the two seed pulses within the electron beam (see Fig. 1).

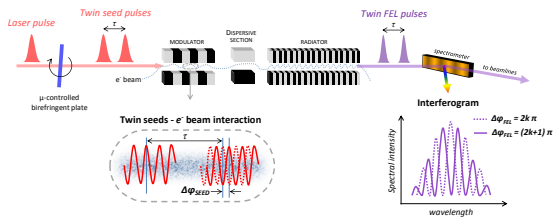

Figure 1: HGHG FEL in the two phase-locked pulses configuration. Two time-delayed seed pulses are created by transmission of a single laser pulse through a birefringent plate. The plate is motorized to precisely control the relative phase $\Delta\phi_{seed}$ between the two carrier waves of the twin seeds, which interact with the relativistic electron beam in the modulator. Image reproduced from [9].

Interferogram Creation and Measurements

Two mutually coherent pulses delayed in time produce a spectral interference pattern [10]. This configuration can be regarded as the temporal equivalent of the Young's double slit interferometer where the time-delayed pulses play the role of the spatially separated slits, and the spectrometer is the equivalent of the far-field screen. The interference arises in the frequency domain instead of the spatial one.

The resulting interferogram is characterized by the presence of interference fringes, the fringe spacing is inversely proportional to the time delay, and the interferogram envelope is a superposition of the spectral envelopes of the two individual pulses. The fringe distribution within the interferogram contains information on the spectral phase difference of the two interfering pulses. The maximum contrast, defined as the ratio between the difference of the maximum and minimum intensity of the spectrogram over the sum of the same quantities, is maximum when the two interfering pulses are identical, with a regular spacing between the fringes. If the two interfering pulses do not have the same amplitude (identical configuration) the fringes' contrast is smeared out and/or one can observe changes in the uniformity of the fringe pattern.

In the experiment, we were interested in the control of the fringe position inside the interferogram envelope. This can be achieved by controlling the carrier-envelope phase difference $\Delta\phi_{FEL}$ between the two FEL pulses.

In the ideal case, for a homogeneous and symmetric interferogram, the relative phase $\Delta\phi_{FEL}$ between the two interfering pulses can be extracted from the position of the fringes as sketched in Fig. 1.

As the FEL emission in a seeded scheme is initiated by the coherent structure imprinted on the electrons by the seed laser itself, we expect that the two FEL pulses obtained using the above scheme will be mutually coherent and that their relative carrier-envelope phase can be precisely controlled. The relative phase between the two FEL pulses is related to the one between the two seeds according to

$$\Delta\phi_{FEL} = n \times \Delta\phi_{seed} + C\,, \qquad (1)$$

where n is the harmonic number. C is a factor that includes the phase contribution due to the electron beam time-dependent energy profile and a phase difference possibly developed during pulses amplification in the radiator.

Interferogram Analysis

Figure 2(a) shows the evolution of the spectral fringes as a function of the rotation angle of the birefringent plate. The minimum rotation step size is $\lambda_{seed}/28.33$, corresponding to $\lambda_{FEL}/5.67$. Figure 2(b) and (c) highlights the fringe displacement for each step. The ability to control the fringe displacement confirms that the phase relationship existing between the twin seed pulses is coherently transferred onto the two FEL pulses. This is a direct consequence of the principle on which a seeded FEL working in the harmonic generation configuration relies.

The analysis of a sequence of shot-to-shot interferograms keeping the twin seed phasing fixed contains complementary information on the stability of the phase locking. The measured fringe instabilities are related to different effects, the main ones were identified to be the shot-to-shot variation of the electron beam properties and the timing jitter between the electron beam and the seed lasers. Changes in the longitudinal electron beam properties experienced by

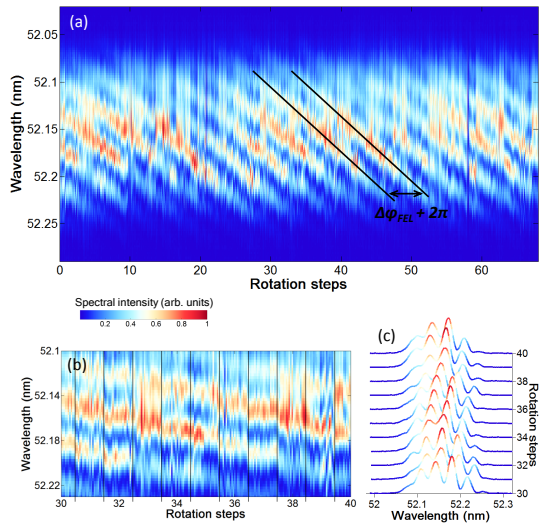

Figure 2: Interferogram from two phase-locked FEL pulses. (a) Evolution of the spectral interference fringes as a function of the rotation angle of the birefringent plate (see Fig. 1). (b) Zoom of the central part. At each rotation step, 20 consecutive single-shot spectra are acquired. (c) Single-shot profiles extracted from (b), one for each rotation step.Image reproduced from [9].

the two time-delayed seed pulses can lead to the emission of non-identical FEL pulses and/or to variations in their relative phase with respect to the one introduced by the twin seeds. The described interferometric method therefore can represent a valuable tool for monitoring the FEL stability and performance.

Using an interferometric setup, we demonstrated phase-locking between two pulses from a seeded FEL and studied the control and the stability of their relative temporal properties. It turns out that the physical process on which an FEL relies preserves the mutual coherence driven by the two seed laser pulses. Finally, we identified the non-ideal electron beam as the main source of the remaining phase instability. In the general context of laser-driven light sources, we proved once again the capability to control and manipulate the light emitted by a seeded FEL [2, 11]. The setup is easy to implement. By extending the FEL output from two to a train of multiple phase-locked pulses, a frequency comb like spectrum could be generated [12]. Moreover, the individual control of each pulse, specifically its spectral phase, can allow a vast range of coherent control applications at short wavelengths, such as quantum state holography [13]. The generation of phase-locked pulses could also be naturally extended to the XUV photon energies generated by FEL-2.

SPIDER RECONSTRUCTION OF FEL PULSES

Single-shot characterization and control of the spectral and temporal features of FEL pulses are fundamental prereq-

uisites for experiments aiming at taking full advantage of the laser-like properties of a seeded FEL. Such a characterization is a challenging task, mainly due to the strong material absorption of the light in the XUV-soft-X-rays wavelength range.

Only few effective techniques have been proposed to measure the duration of a femtosecond short-wavelength SASE pulse [14, 15]. In the following we demonstrate the possibility to reconstruct, both in the temporal and spectral domains, the envelopes and phases of a pulse generated by a seeded FEL using the spectral phase interferometry for direct electric-field reconstruction (SPIDER) method [16].

Generation of the Interferogram

As mentioned, the electron-beam energy is generally characterized by a time-dependent profile. If two seed replicas separated by a time interval τ overlap with a quadratic zone of the $\gamma(t)$ curve, two FEL pulses, separated by the same temporal distance of the two seeds, are generated. The FEL pulses are also shifted in frequency by a shear Ω depending on the derivative of the quadratic curvature of the beam energy profile. If the electron beam properties are sufficiently homogeneous, the generated FEL pulses have equal intensities and temporal phases, satisfying the condition for the application of the SPIDER algorithm.

In the experiment the core of the electron beam, corresponding to the highlighted region in Fig. 3(a), is characterized by a dominant quadratic curvature of about 6.5 MeV/ps^{-2} in the beam energy profile $\gamma(t)$.

The seed replicas to generate the twin FEL pulses were obtained by splitting the pulse of the third harmonic of a Ti:Sa laser by means of adjustable polarization rotation and a birefringent plate, similar to the one described in the previous experiment. As the seeded FEL pulse properties critically depend on the seed laser properties, we manipulated the seed temporal duration and chirp using an adequate calcium fluoride lamina and/or an optical compressor based on transmission gratings. The seed wavelength was 261 nm and the replica separation $\tau = 230$ fs. The FEL was operated at $n = 5$ (i.e., 52.2 nm). At the end of the radiator, this results in the generation of two FEL pulses separated in time by τ and shifted by a frequency Ω, which is directly proportional to the amount of electron-energy quadratic chirp.

The twin FEL pulses yield a spectral interferogram, cfr. Fig. 3(c) on which the SPIDER algorithm relies that was recorded using on the on-line PADReS photon spectrometer [17]. As shown in Fig. 3(b), the interferograms evolve as a function of the relative delay between the seed replicas and the electron beam. Vertical cuts of the map provide single-shot interferograms, see Fig. 3(c). As expected, the central wavelength of the inteferograms generated by the electrons in the quadratic region displays a linear shift. The good contrast of the interference fringes is a clear indication of the similarity of the interfering pulses. The measured shift between spectra separated by the temporal distance τ corresponds to the spectral shear Ω. For the experiments the maximum possible value of τ is determined by the extension of the highlighted region in Fig. 3, where the electron-beam energy profile is characterized by a dominant homogeneous quadratic dependence. The shear Ω is then determined by the amount of such a quadratic chirp. Outside this region, higher-order nonlinear terms become non-negligible. This makes it impossible to generate (almost) identical FEL pulses and, therefore, apply the SPIDER reconstruction. In our working conditions, $\Omega = 1.7 \times 10^{13}$, which corresponds to $\Delta\lambda = 2\pi\Omega/\lambda^2 \simeq 0.025$ nm ($\lambda = 52.2$ nm).

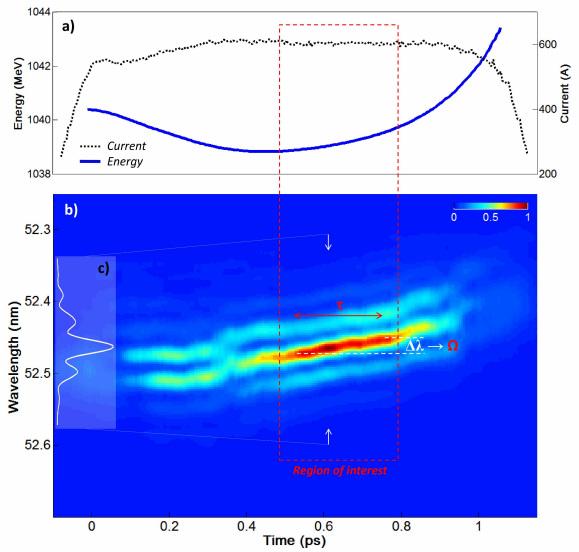

Figure 3: Generation of the FEL interferogram. (a) Energy and current time-dependent profiles of the FERMI electron beam (the bunch head comes at smaller times). In the highlighted region, the energy profile is characterized by a dominant and constant quadratic term. (b) FEL intereferograms as a function of the temporal position of the leading seed pulse with respect to the electron beam. Image reproduced from [1].

Analysis of the Interferogram

The inteferograms in the region of interest highlighted in Fig. 3(b) were used to carry out the SPIDER analysis of the FEL pulse. The reconstructed temporal phase profile has a positive curvature which corresponds to a dominant positive linear frequency chirp on the pulse. This is consistent with the parameters of the machine, as both the electron beam energy and the seed pulses were characterized by a positive chirp. The obtained spectral bandwidth and pulse duration are, respectively, 6.3×10^{-2} nm and 71 fs (FWHM). The value of the bandwidth is very close (within a few per cent) to the one obtained by directly measuring the spectrum of a single FEL pulse, generated by one of the seed replicas. According to the existing theory [18], the FEL pulse duration, Δt_{FEL}, is expected to scale approximately as $\Delta t_{seed} \times n^{-1/3}$, where Δt_{seed} is the duration of the seed pulse. Using the parameters of the experiment the expected FEL pulse duration is 73.7 fs (FWHM), in good agreement

with the reconstructed value. Notice that the time-bandwidth product, supposing a Gaussian profile of the pulse, is a factor 1.1 above the Fourier limit. The reproducibility of the presented method is demonstrated by comparing the reconstructions obtained for different positions in the region of interest and for different FEL shots. The observed fluctuations in bandwidth and pulse duration are smaller than 10%, confirming also the stability of the machine.

Summary

The method we have implemented allows to carry out single-shot spectro-temporal characterizations of femtosecond XUV pulses produced by a seeded FEL. Our measurements also constitute the first direct evidence of the temporal coherence of a seeded FEL pulse in the XUV wavelength range. The comparison between the results for the two different seed conditions paves a way to fully control the FEL spectral and temporal properties by properly adjusting the seed laser chirp. This opens the way to the generation of flat-phase Fourier-limited femtosecond pulses in the XUV region using a seeded FEL, as we will see in the following. The results are in agreement with previously developed theory. The described approach is independent of the wavelength of the radiation and can therefore be implemented on present and future facilities in order to monitor and shape the properties of a seeded FEL pulse.

SPECTRO-TEMPORAL SHAPING OF SEEDED FEL PULSES

By taking inspiration from the results reported in the previous section, we carried out a series of experiments aimed at demonstrating the possibility of fully controlling the spectro-temporal content of FEL XUV pulses by properly tuning the seed laser operating parameters. The results constitute the first experimental evidence of Fourier limited pulses from an FEL in the XUV spectral range. The possibility of tailoring the spectro-temporal content of intense short-wavelength pulses represents the first step towards efficient nonlinear optics in the XUV to x-ray spectral region and will enable precise manipulation of core-electron excitation using, e.g., coherent quantum control.

How to Control the FEL Pulse Shape

The FEL output at the n$^{\text{th}}$ harmonic is driven by the electron bunching factor b_n, that can be written as [3, 18]

$$b_n(t) = \mathrm{e}^{-n^2B^2/2} J_n(-nBA(t)) \exp(in(\phi_s(t)+\phi_e(t))), \quad (2)$$

where B is the dispersive section strength [18], J_n is the n^{th} order Bessel function, and $A(t)$ is the time-dependent energy modulation (normalized to the electron energy spread σ_γ), which is proportional to the envelope $a_0(t)$ of the seed laser electric field

$$a(t) = a_0(t)\sin(\omega_0 t + \phi_s(t)), \quad (3)$$

ω_0 being the central frequency. The exponent in the last factor, where $\phi_e(t) = (B/\sigma_\gamma)E(t)$, accounts for the slowly varying phase of the seed, i.e. $\phi_s(t)$, and for a possible time-dependent energy profile of the electron beam. As the microbunched beam is injected into the radiator it starts emitting coherent light. Initially the electron beam is rigid and the FEL electric field is directly proportional to the bunching factor in Eq. (2). Before saturation occurs, the shape of the field envelope is preserved despite amplification in the radiator. However, a small additional phase $\phi_a(t)$ due to the amplification process is introduced [4, 5, 7], so that the total FEL phase becomes

$$\phi_{FEL}(t) = n[\phi_s(t) + \phi_e(t)] + \phi_a(t)\,. \quad (4)$$

The above equations provide the basis for FEL pulse shaping through the manipulation of the seed envelope $a_0(t)$ and phase $\phi_s(t)$.

Both the electron beam time-dependent energy profile and the phase developed during amplification affect the pulse properties [4, 5, 7, 18]. However, these effects can be fully compensated for by properly tuning the temporal phase of the seed laser. For the cases considered here, it suffices to expand each of the individual phase contributions $\phi_s(t)$, $\phi_e(t)$, and $\phi_a(t)$ into a power series in time up to the second order. While a linear-term coefficient $d\phi(t)/dt$ results in an absolute frequency (wavelength) shift [6], a quadratic-term coefficient $d^2\phi(t)/dt^2$ gives rise to a linear frequency chirp in the pulse [3]. A suitable seed laser chirp can then be used to counter the combined effects due to the electron beam quadratic energy curvature and the chirp developed during amplification.

First, the bunching envelope, generated here by a Gaussian seed, can be modified by changing the strength B of the dispersive section. With increasing B, the bunching develops modulations as a function of time (Eq. (2)) due to the process of electron overbunching and rebunching [19, 20], leading to a pulsed structure. As emphasized above, the FEL pulse temporal shape directly corresponds to the bunching envelope. Second, manipulating the FEL temporal phase using a chirped seed, leads to a drastic modification of the FEL spectral content. While the spectral map (spectrum versus B) of a significantly chirped FEL pulse directly corresponds to its temporal map [21, 22], a Fourier limited pulse with a flat temporal phase shows a distinctively different spectral signature.

Results

We verified the predictions and demonstrated the possibility of controlling the spectro-temporal content of the FEL pulses with dedicated experiments. As described before, we can manipulate the seed laser chirp either by introducing a proper lamina and/or by using a grating-based optical compressor.

Figure 4(a) shows the measured spectral map if a strong positive chirped seed laser (5.9×10^{-5}rad/fs^2) is used to seed the FEL, that will exhibit a corresponding positive frequency chirp.

One can see that the FEL spectrum develops intensity modulations as B is increased, which directly correspond to the intensity modulations in the temporal domain. Excellent agreement between experiment and theory (inset) demonstrates that, despite amplification in the radiator, the FEL pulse envelope is preserved, justifying the use of Eqs. (2) and (4) to describe the spectro-temporal content of FEL light.

The next experiment, Fig. 4(b), was performed with a moderate positive chirp on the seed laser (6.7×10^{-5}rad/fs^2). Because the total FEL chirp is not high enough to satisfy the condition for the spectro-temporal equivalence [22], the central part of the spectral map is significantly modified with appearance of intensity islands. Again, a remarkably good correspondence is obtained between experiment and theory.

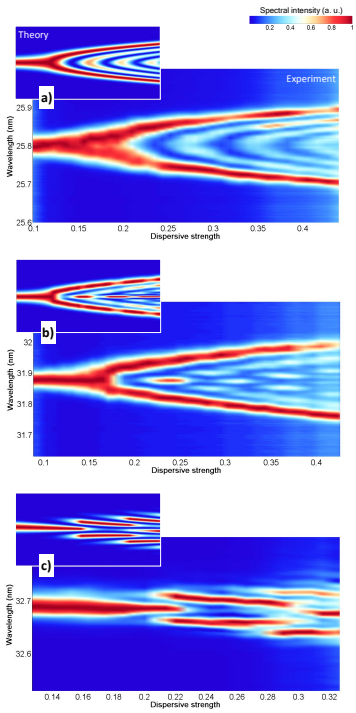

Figure 4: FEL pulse spectra as a function of the dimensionless dispersive strength for three different conditions of the linear frequency chirp on the seed laser. (a) Significant positive chirp, (b) moderate positive chirp, and (c) slight negative chirp for chirp compensated FEL pulses. Insets are theoretical spectral maps reproduced using Eqs. (2) and (4) in the spectral domain. Image reproduced from [2].

Based on the two spectral signatures in Figs. 4(a) and 4(b), the next set of experiments was carried out by putting a negative chirp rate on the seed (-2.0×10^{-5}rad/fs^2). A strong modification of the spectral content versus B with respect to the previous two cases is seen in Fig. 4(c), confirming the extremely high sensitivity of the spectral maps to the FEL phase. Experimental data once again fit well with calculations reported in the inset of the same figure.

Remarkably, the spectral signature corresponds to that of a Fourier limited pulse with a flat temporal phase. The negative chirp rate on the seed compensates the positive chirp in the electron beam energy which was in the experiment ~12 MeV/ps^2, measured at the end of the LINAC, and the chirp developed during the amplification stage. More precisely, because the phase contribution from the electron beam $\phi_e(t)$ is a function of B, the FEL chirp rate varies linearly from about -1 to 9 $\times10^{-5}$rad/fs^2 in the range of dispersive strengths used in Fig. 4(c), going through zero at B ~ 0.14, where full chirp compensation is achieved.

SUMMARY

The experimental spectral maps in Fig. 4 and their striking agreement with theory, Eqs. (2) and (4), imply that we are able to fully manipulate the FEL output pulse by finely tuning the seed laser envelope and phase. The dispersive section can be used as an additional tuning knob, e.g. an FEL pulse train with a fixed phase relationship can be obtained by simply increasing the strength of the dispersive section. Our results demonstrate that, by adjusting the seed laser phase, a controllable amount of linear frequency chirp can be transferred to the FEL pulse, which can enable, e.g., chirped pulse amplification [23] on an FEL.

A careful tuning allows generation of Fourier limited pulses with a flat temporal phase. Such pulses are typically used as references in the field of coherent quantum control. Our results therefore enable full spectro-temporal shaping of intense ultrashort pulses in the XUV to soft-x-ray region using methods similar to the ones developed in the visible spectral region [24].

REFERENCES

[1] G. De Ninno *et al.*, *Nat. Commun.* 6, 9075, 2015.

[2] D. Gauthier *et al.*, *Phys. Rev. Lett.* 115, 114801, 2015.

[3] D. Ratner *et al.*, *Phys. Rev. ST Accel. Beams* 15, 030702, 2012.

[4] A.A. Lutman *et al.*, *Journal of Physics* A: Mathematical and Theoretical 42, 085405, 2009.

[5] A. Marinelli *et al.*, *Phys. Rev. ST Accel. Beams* 13, 070701, 2010.

[6] T. Shaftan and L.-H. Yu, *Phys. Rev.* E 71, 046501, 2005.

[7] J. Wu *et al.*, *J. Opt. Soc. Am.* B 3, 484–495, 2007.

[8] E. Allaria *et al.*, *Nature Photonics* 10, 699–704, 2012.

[9] D. Gauthier *et al.*, *Phys. Rev. Lett.* 116, 024801, 2016.

[10] J. Goodman, *Introduction to Fourier Optics*, Robert & Company Publishers, 2005.

[11] P.R. Ribič *et al.*, *Phys. Rev. Lett.* 112, 203602, 2014.

[12] S. T. Cundiff and Y. Jun, *Rev. of Mod. Phys.* 75, 325, 2003.

[13] C. Leichte *et al.*, *Phys. Rev. Lett.* 80, 1418–1421, 1998.

[14] I. Grguras *et al.*, *Nat. Photon.* 12, 852–857, 2012.

[15] C. Behrens *et al.*, *Nat. Commun.* 5, 4762, 2014.

[16] C. Iaconis and I. A. Walmsley, *Opt. Lett.* 23, 792–794 ,1998.

[17] C. Svetina *et al.* Proc. SPIE 8139, 81390J, 2011.

[18] G.V. Stupakov, SLAC Internal Report 94, 14639, 2011.

[19] M. Labat *et al.*, *Phys. Rev. Lett.* 130, 264801, 2009.

[20] D. Xiang *et al.*, *Phys. Rev. Lett.* 113, 184802, 2014.

[21] G. De Ninno *et al.*, *Phys. Rev. Lett.* 110, 064801, 2013.

[22] D. Gauthier *et al.*, *Phys. Rev.* A 88, 033849, 2013.

[23] D. Strickland and G. Mourou, *Optics Commun.* 3, 219–221, 1985.

[24] A. M. Weiner, *Optics Comm.* 284, 3669–3692, 2011.